Evidence of abyssal eddies in the Brazil Basin

Georges Weatherly
Department of Oceanography, Florida State University, Tallahassee, Florida, USA

Michel Arhan and Herle Mercier
Laboratoire de Physique des Océans (CNRS-IFREMER-UBO), IFREMER, Plouzané, France

William Smethie Jr.
Lamont-Doherty Earth Observatory, Palisades, New York, USA

Received 21 September 2000; revised 15 August 2001; accepted 23 August 2001; published 18 April 2002.

[1] We report evidence of two deep cyclonic and two deep anticyclonic submesoscale eddies from World Oceanographic Circulation Experiment hydrographic casts made in the Brazil Basin. We infer that three of these were likely formed in or near the Deep Western Boundary Current (DWBC) of North Atlantic Deep Water (NADW), and thus had traveled eastward after formation. These eddies appear to be a new way for transporting NADW away from the DWBC to the ocean interior. One of the apparent cyclonic eddies appeared to be laterally in contact with one of the anticyclonic eddies. About 10 days later an attempt was made to resample the apparent eddies that had been in contact. These observations, although limited, are interpreted to indicate that they survived the encounter, that the cyclonic eddy had now moved to be beneath the anticyclonic one with each being somewhat thinner, and that they produced a new anticyclonic eddy by partially merging. Deep float observations [*Hogg and Owens*, 1999] partially support the second inference. *INDEX TERMS:* 4520 Oceanography: Physical: Eddies and mesoscale processes; 4532 Oceanography: Physical: General circulation; 4536 Oceanography: Physical: Hydrography; *KEYWORDS:* eddies, Deep Western Boundary Current, eddy merging

1. Introduction

[2] Anticyclonic, submesoscale coherent eddies are fairly common in the ocean [e.g., *McWilliams*, 1985]. These are convex lenses of anomalous water found at middepths with radii somewhat less than the internal Rossby radius of deformation. The best known and studied are Meddies of Mediterranean water [e.g., *Bower et al.*, 1997] found in the North Atlantic subtropical gyre. They have radii 30–60 km, are 200–1000 m thick, are centered at about 1000 m depth, are long-lived (order a year), have orbital speeds about 30 cm s^{-1}, and have translational velocities of about 3 cm s^{-1}, often toward the southwest [*Bower et al.*, 1997; *Richardson and Tychensky*, 1998]. In the North Atlantic subtropical gyre, similar eddies of Labrador Seawater are found below the thermocline [*Elliot and Sanford*, 1986]. Red Seawater eddies (Reddies) are found in the Indian Ocean [*Shapiro and Meschanov*, 1991]. Examples of anticyclonic eddies of Chuckchi Seawater in the Beaufort Sea in the western Arctic Ocean have also been reported [*D'Asaro*, 1988].

[3] Cyclonic, submesoscale eddies are rarer but are not uncommon. *Colin de Verdière et al.* [1989] and *Schauer* [1989] collectively found 11 examples below the thermocline in the central and eastern North Atlantic between 43° and 49°N. Compared to Meddies, they had comparable radii, swirl speeds, and translational speeds but were deeper: cores at ≈1700–2000 m depth; were thicker: ≈1–2 km thick; and (of course) had concave lenses. *Paillet et al.* [1998] reported six similar concave features farther to the south between 40° and 43°N. In the South Atlantic, *Richardson and Fratantoni* [1999] observed a cyclonic eddy moving to the east for 3 months and then to the west for a comparable period. It was found around 10°S in the western Brazil Basin, and they thought it was shed from the Deep Western Boundary Current (DWBC) of North Atlantic Deep Water (NADW). *Hogg and Owens* [1999] also reported a deep float being trapped in a cyclonic eddy in the Brazil Basin. We shall see later that this float may have been set in one of the deep features reported here.

[4] The subject of eddy merging has received much attention and is not limited to submesoscale eddies but includes larger eddies as well [cf. *Nof and Dewar*, 1994, and references therein]. As pointed out by *Nof and Dewar* [1994], essentially all the studies are of eddies and rings of the same sign vorticity, and most are of eddies of like density. Observations of the interaction of two large eddies of different densities indicate that they can realign as two vertically stacked eddies e.g., *Cresswell*, 1982]; from this, *Nof and Dewar* [1994] concluded that density differences of the eddies may play a role in how they interact. The finding of vertically stacked Meddies [*Ambar et al.*, 1991] suggests that Meddies of differing densities may realign vertically

0148-0227/02/2000JC000648$09.00

after they come into contact. We are unaware of observations of the interaction of a deep cyclonic eddy with an anticyclonic one.

[5] We report observations of some unusual features sampled in the Brazil Basin in the South Atlantic during two World Ocean Circulation Experiment (WOCE) hydrographic sections. We will later identify these features as deep cyclonic or anticyclonic eddies (hereinafter ceddies and aeddies, respectively), although only one station was made in each deep eddy. As the station spacing was 55 km, we can only say that the eddy radii were lower than, or equivalent to, this value, and with the Rossby radii of deformation for this region comparable to this distance [*Houry et al.*, 1987] the structures may be regarded as submesoscale coherent vortices. As noted above, submesoscale vortices are not unusual in the oceans, and with the recent studies of the previously relatively poorly sampled Brazil Basin accomplished during the Deep Basin Experiment component of WOCE [e.g., *Hogg et al.*, 1996] one might expect some reports of submesoscale deep eddies there. Indeed, as noted earlier, *Richardson and Fratantoni* [1999] and *Hogg and Owens* [1999] reported ceddies there from deep float trajectories. We suspect we too have sampled some eddies in the Brazil Basin, but because of the spacing of the stations, this cannot be validated.

[6] One of the unusual features was observed in the southwestern part of the basin during WOCE hydrographic section A17 (hereinafter referred to as A17 and shown in Figure 1). In the property sections of A17 the feature is conspicuous; for example, in the θ section of Figure 2a its lower part is the cold core-like feature in the lower water column at 26°S. (Some of the figures in this text, including Figure 2a, reflect an initial interest of one of us (G. W.) in near-bottom (depths $\leq$ 3600 m) processes in the Brazil Basin by the choice of contouring nearer the bottom (Figure 2a) and by what is sometimes plotted (e.g., σ_4 in Figure 4a)). During the 19°W portion of the WOCE hydrographic section A15 (hereinafter referred to as A15W and shown in Figure 1) another unusual feature was observed, this time in the central eastern portion of the basin around 18°S. It too is a conspicuous feature in the A15W sections, but it is more complicated than what was seen at A17 station 84. For example, in the θ section (Figure 2b) its lower portion appears as a cold core-like feature at station 82 (similar to what was seen at A17 station 84); however, it appears as a warm core-like feature to the north at station 81. Later, we will suggest that it was likely composed of a ceddy (at A15W station 82) adjacent to and/or in contact with an aeddy (at A15W station 81). During the $\approx$18°S portion of A15 (hereinafter referred to as A15S and shown in Figure 1), which began shortly after the completion of A15W, an attempt was made to resample the unusual feature seen on A15W. Two unusual features, adjacent to and in contact with each other, were seen to the east of 18°W, one at station 110 and the other at station 112, with the former partially resolved because of limited sampling to the east (e.g., Figure 2c). Later, we suggest that one of them may have been two features, the remnants of the eddies that were seen at A15W stations 81 and 82, one on top of the other, and the other may have been a new aeddy formed by their partial merger. Section 2 describes the features observed on A17 and on A15W. Section 3 considers what was seen on A15S. Section 4 considers where the features seen on A17 and A15W may have been formed. Section 5 summarizes and discusses.

2. Description of What Was Seen on A17 and A15W

2.1. A17

[7] The unusual feature observed during the A17 survey is evident in the σ, S, and O_2 sections shown in Figure 3 at station 84 (1949–2229 UTC; 2 February 1994; 26°11′S, 35°34′W). In this study we will call a feature a ceddy (aeddy) if its density field shows concave (convex) lens structure, if its S and O_2 sections indicate cores near the density core, and if the potential temperature θ-S properties of the cores are anomalous relative to the surrounding water. In terms of density (Figures 3a and 4a) the feature displays a concave lens structure for 1500 m $\leq$ depths $\leq$ 4080 m depth (the bottom), and associated with its density core at $\approx$2500 m depth, there is an S core centered at $\approx$2320 m depth (Figure 3b) and an O_2 core centered at $\approx$2470 m depth (Figure 3c). The θ-S properties of the feature (Figure 4b) indicate anomalous water properties for $45.65 \leq \sigma_4 \leq 45.78$ (Figure 4b), which corresponds to 2210 m $\leq$ depths $\leq$ 2650 m (Figure 4a). (Hereinafter, that portion of an unusual feature that has anomalous water as indicated in θ-S plots is called a bolus.) Thus we hereinafter call the feature a ceddy (recognizing, as noted earlier, it is too poorly sampled to be clearly resolved as such) and note that its bolus is about 440 m thick, while density indicates it is about 2.6 km thick.

[8] The geostrophic velocity sections with a level of no motion (LNM) at the bottom indicate a maximum swirl speed of $\approx$14 cm s^{-1} (Figure 4c) for this ceddy. (This speed would be larger if the ceddy's radius were smaller than the $\approx$55 km dictated by the station spacing.) The velocity section with the LNM at σ_2 = 36.70, the approximate interface between Antarctic Intermediate Water (AAIW) and NADW (not shown) also yields a ceddy centered at the same depth. However, the ceddy is then sandwiched between an anticylone above and below. Taking the LNM at σ_4 = 45.87, the approximate interface between NADW and Antarctic Bottom Water (AABW) (not shown), yields a qualitatively similar situation as for the LNM at σ_2 = 36.70 case. Later, we will see that the ceddy was probably formed at or near the DWBC and of NADW. This, together with the results of *Weatherly et al.* [2000], which show that this DWBC at 18°S is part of a flow extending upward into AAIW and downward into AABW, leads us to think that Figure 4c is a more representative velocity section than the ones with a LNM at σ_2 = 36.70 or at σ_4 = 45.87.

[9] We note that our LNM choice (at the bottom) and that of *Wienders et al.* [2000] in the same region of A17 of σ_2 = 36.83 (which is near, but about 320 m deeper than, the σ_2 = 36.70 level between AAIW and NADW discussed in the previous paragraph) yield velocities in the depth range 150–250 m, which differs from those inferred by the shipboard acoustic Doppler current profiler (ADCP) at A17 station 84 over the same depth range by $\approx$12 cm s^{-1} (the former) and by $\approx$8 cm s^{-1} (the latter), where positive values indicate flow toward South America. However, the

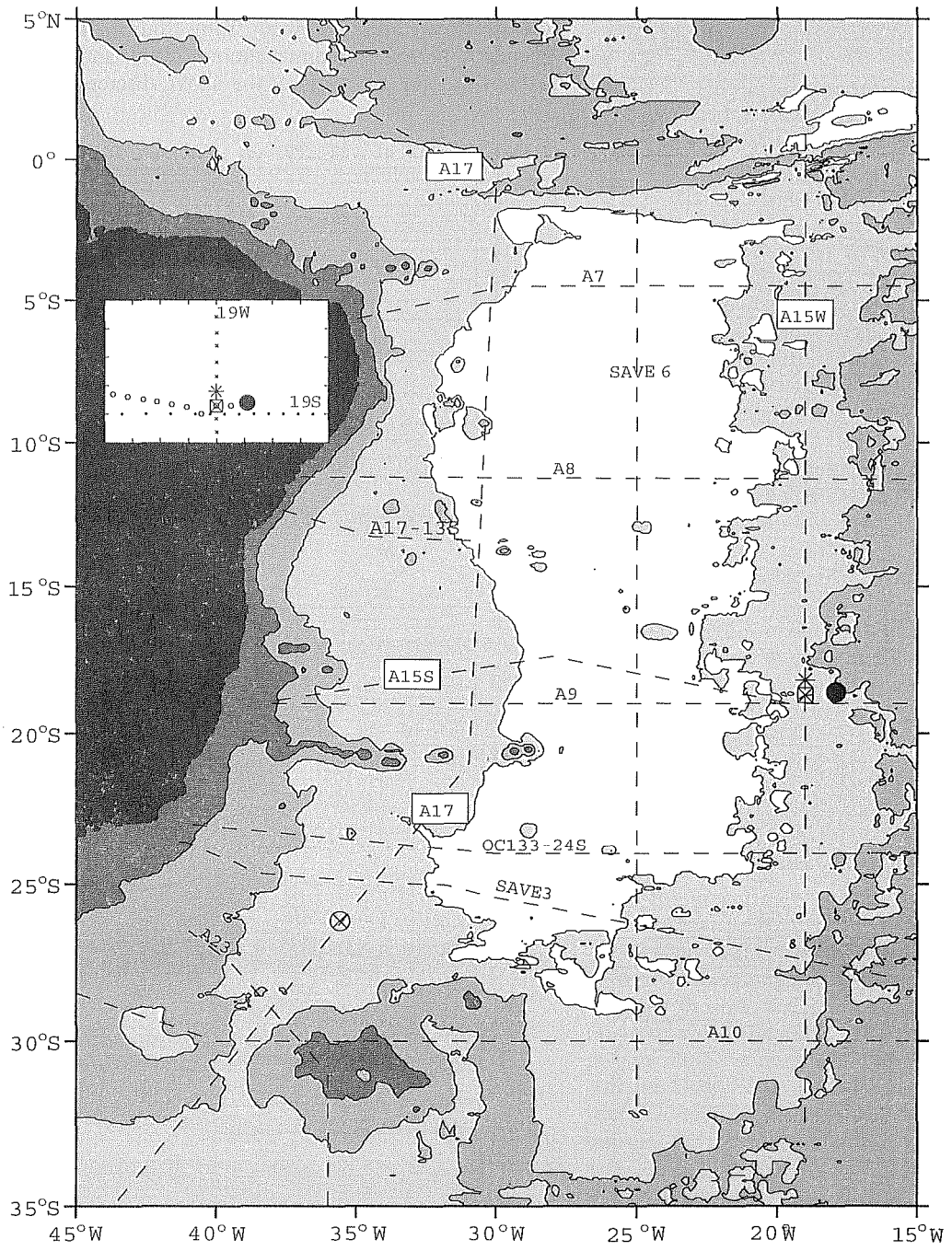

Figure 1. Chart of the Brazil Basin with 2000, 4000, and 5000 m depth contours drawn, the darkest contour being land. The location of A17 station 84 is the open circle with an X inside, that of A15W station 81 is the asterisk, that of A15W station 82, which is also the location of A15S station 112, is the open square with an X inside, and that of A15S station 110 is the large solid circle. The insert shows where A15W and A15S (and A9) intersect with A15W stations (crosses), A15S stations (open circles), and A9 stations (dots) and where A15W stations 81 and 82 and A15S stations 110 and 112 are labeled as in the chart. Some of the Bahia Seamounts, not labeled, are shown surrounding the "A17-13S" identifier. Hydrographic sections discussed in the text are the labeled dashed lines: A17 (WOCE A17, a quasi-meridional section in the western Brazil Basin), A15W (the portion of WOCE A15 along 19°W), A15S (the portion of WOCE A15 nominally along 18°S), A7 (WOCE A7, a zonal section along 4.5°S), A8 (WOCE A8 along 11°S), A17-13S (the portion of WOCE A17 along 13°S), A9 (WOCE A9, a zonal section along 19°S), OC133-24S (the portion of Oceanus 133 nominally along 24°S), SAVE3 (the quasi-zonal South Atlantic Ventilation Experiment (SAVE) section along ≈25°S), A23 (WOCE A23), and A10 (WOCE A10, along 30°S).

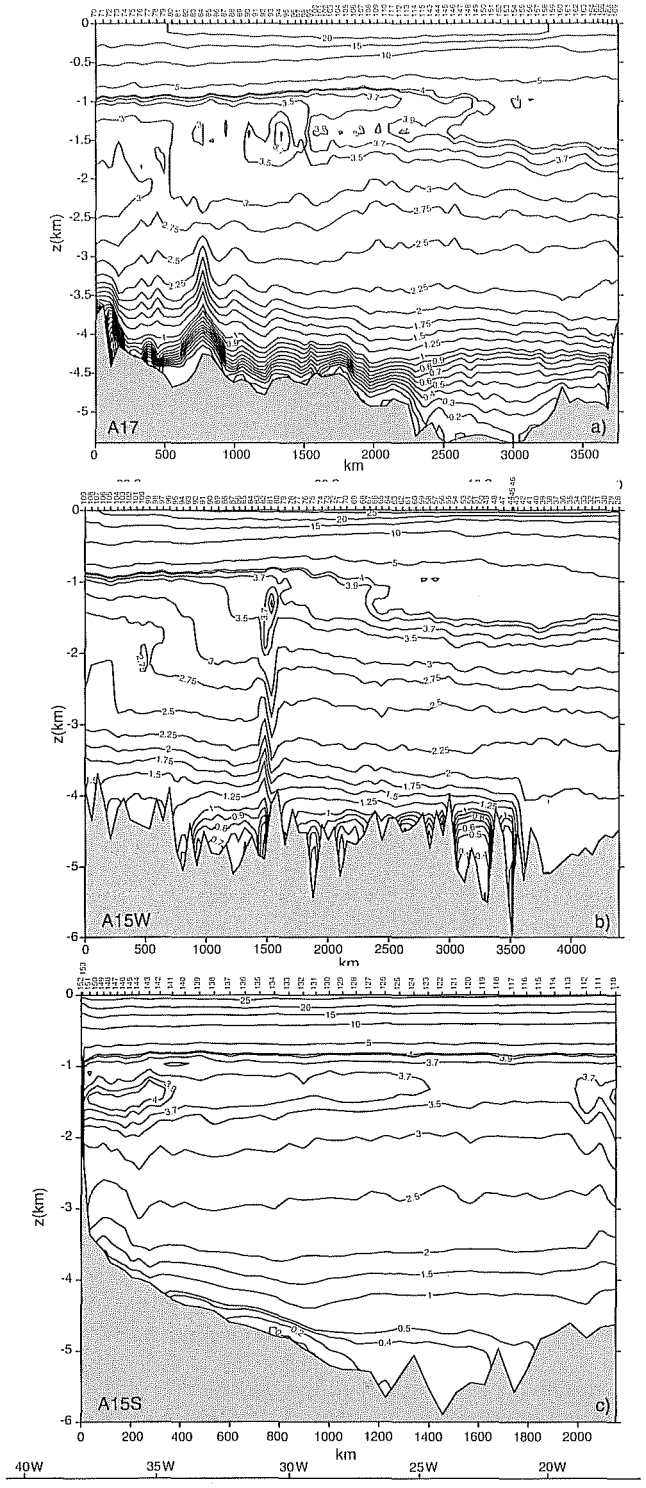

Figure 2. (a) Brazil Basin portion of the A17 quasi-meridional θ section. Of interest is the cold-core feature at 26°S extending from the bottom upward to about 2500 m depth. (b) The A15 19°W θ section. The feature considered is seen at 18°–19°S extending from the bottom to about 1000 m depth and appears to have a cold-core structure (station 82) adjacent to a warm-core structure (station 81). (c) The A15 18°S θ section. The features considered are east of 19°W at stations 110 and 112 starting at about 1 km depth going to depths of about 3–4 km.

A17 shipboard ADCP inferred velocities were biased toward flow directed away from South America (N. Wienders, personal communication, 2001), and this could perhaps account for some of the above discrepancies. It is

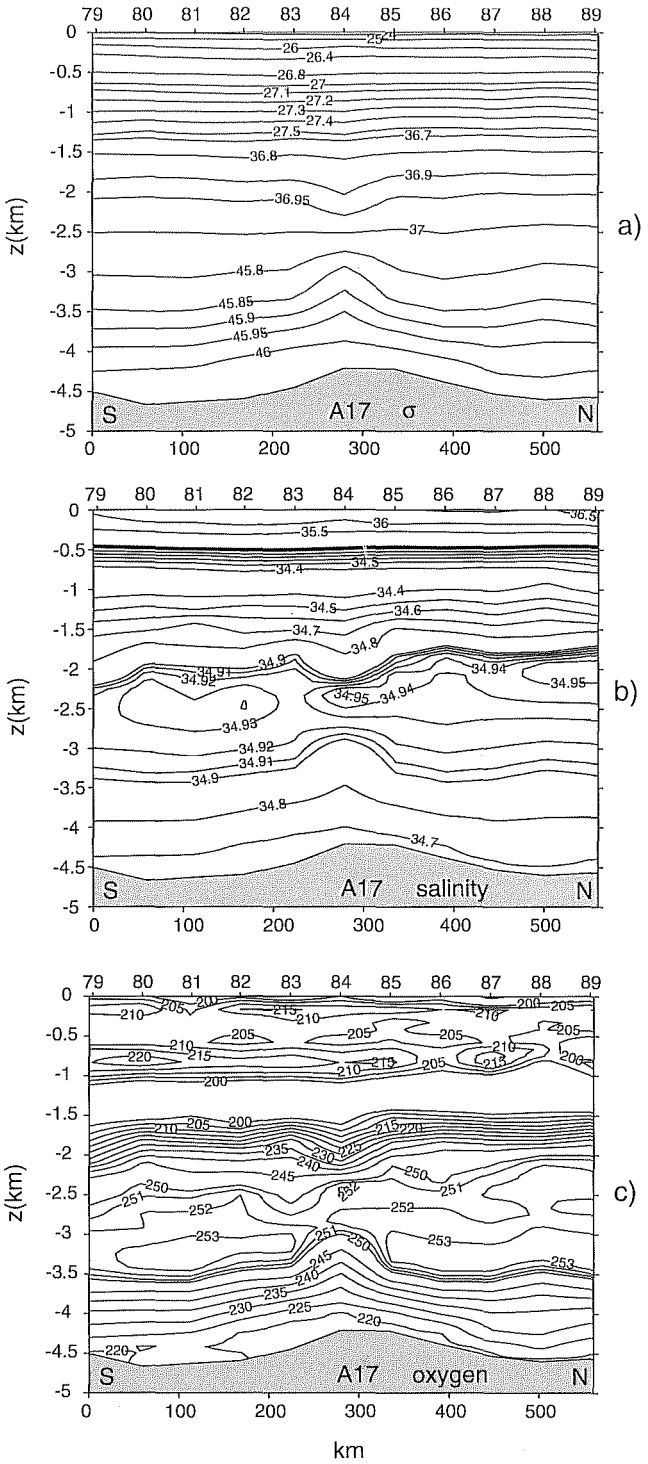

Figure 3. (a) Density in kg m^{-3}, (b) S in psu, and (c) O_2 in μmol kg^{-1} sections for A17 stations 79–89; the feature is at station 84. In the density plot σ_0, σ_2, and σ_4 are plotted for 0 < depth ≤ 1000 m, 1000 m < depth ≤ 3000 m, and 3000 m < depth < bottom, respectively. N and S in the bottom corners denote north and south.

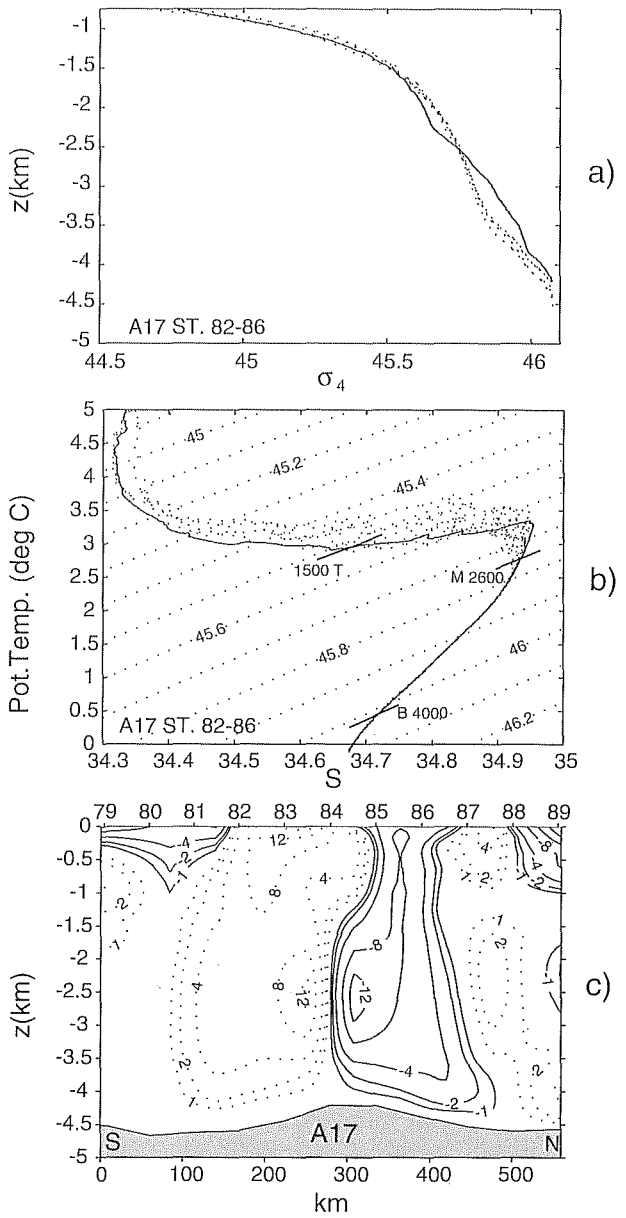

Figure 4. (a) The σ_4 versus depth for the stations 82–86 of A17 with the solid line being station 84's values. A ceddly-like feature is shown (as in Figure 3a) at station 84, which extends upward to about 1500 m depth and downward to about 4080 m depth (the bottom) with a density core at about 2600 m depth, and allows depths to be determined in Figure 4b. (b) The θ-S plots for the stations shown in Figure 4a with station 84's values being the solid line. The σ_4 contours are shown. T, M, and B denote the top, center, and bottom of the ceddy, and the adjacent numbers are the corresponding depths in meters. (c) Geostrophic velocity section for stations 82–86 of A17. Values are in cm s^{-1} and positive into the plane of the figure. S and N in the bottom corners denote south and north. The level of no motion is at the bottom.

not apparent to us that reference velocities inferred from shipboard A17 ADCP values are more suitable than those used here or by *Wienders et al.* [2000], at least in the vicinity of station 84.

2.2. A15W

[10] In terms of density the portion of the unusual feature at A15W station 82 (0002–0410 UTC; 28 April 1994; 18°43′S, 19°0′W) is ceddy-like, extending upward to ≈1200 m depth and down to the bottom at ≈4500 m depth with a (density) core at ≈2300 m depth (Figures 5a and 6a). Similarly, the portion of the feature at A15W station 81 (1405–1657 UTC; 28 April 1994; 18°12'S, 19°0′W) is aeddy-like, extending upward to ≈800 m depth and downward to ≈4000 m depth with a (density) core at ≈1600 m depth (Figures 5a and 6a). In terms of S the feature has a reclining pear-shaped core centered at ≈1900 m depth at station 81(Figure 5b), and in terms of O_2 it has a core centered at ≈2200 m depth at station 82 (Figure 5c)

[11] Examining θ-S plots (Figure 6b) indicates that at A15W station 82 there is a bolus for $45.45 \leq \sigma_4 \leq 45.80$, which corresponds to 1465 m ≤ depths ≤ 2600 m (Figure 6a), approximately the upper portion of this ceddy-like feature (Figures 5a and Figure 6a). The same plots indicate that at A15W station 81 there is a bolus for $45.42 \leq \sigma_4 \leq 45.87$, which corresponds to 1130 m ≤ depths ≤ 3775 m, and that this bolus has different water characteristics (higher θ and S) than the one at A15W station 82. Also, comparing the θ-S properties of the bolus of the A17 ceddy (Figure 4) to that seen at A15W stations 81 and 82 (Figure 6b) shows they are different, suggesting a different source region for each. The bolus thickness of the ceddy-like feature at station 82 is 2.6 times thicker than that of the A17 station 84 ceddy and 0.4 thinner than that of the aeddy-like feature at station 81.

[12] Note that in the A15W section the water properties for 1500 m ≤ depths ≤ 3700 m north of the unusual feature at stations 81 and 82 appear different from those to the south (Figures 2b, 5b and 5c). This is reflected in the θ-S curves (Figure 6b) for the corresponding $45.55 \leq \sigma_4 \leq 45.90$. The stations to the north cluster about a common cooler, fresher range of values (stations 77–80 in Figure 6b), and those to the south cluster about a warmer, saltier range of values (stations 83–87 in Figure 6b). This depth/density range corresponds approximately to where North Atlantic Deep Water (NADW) is found in the Brazil Basin [e.g., *Durrieu de Madron and Weatherly*, 1994]. Thus the unusual feature is found at a front separating a cooler, less salty, older NADW type to the north from a warmer, saltier, and younger NADW type. We interpret this water to the south of this front as part of the eastward flowing Namib Col Current [*Speer et al.*, 1995] and that to the north as part of a westward flow reported by *Reid* [1989].

[13] The geostrophic velocity section with the LNM at the bottom (Figure 6c) gives a maximum swirl speed of 27 cm s^{-1} for the southern half of the ceddy-like feature at station 82 and 17 cm s^{-1} for the northern half of the aeddy-like feature at station 81. Where the two eddy-like features reinforce, the maximum swirl speed is 43 cm s^{-1}. The ceddy-like feature at station 82, like the one at A17 station 84, is indicated as having anticyclones above and below if the LNM is taken at $\sigma_2 = 36.70$ (not shown) or $\sigma_4 = 45.87$ (not shown). Shipboard ADCP records from A15 are unavailable.

[14] So far, the southern portion of the feature at A15W station 82 has been called ceddy-like and the other portion at station 81 has been called aeddy-like. At station 82 there

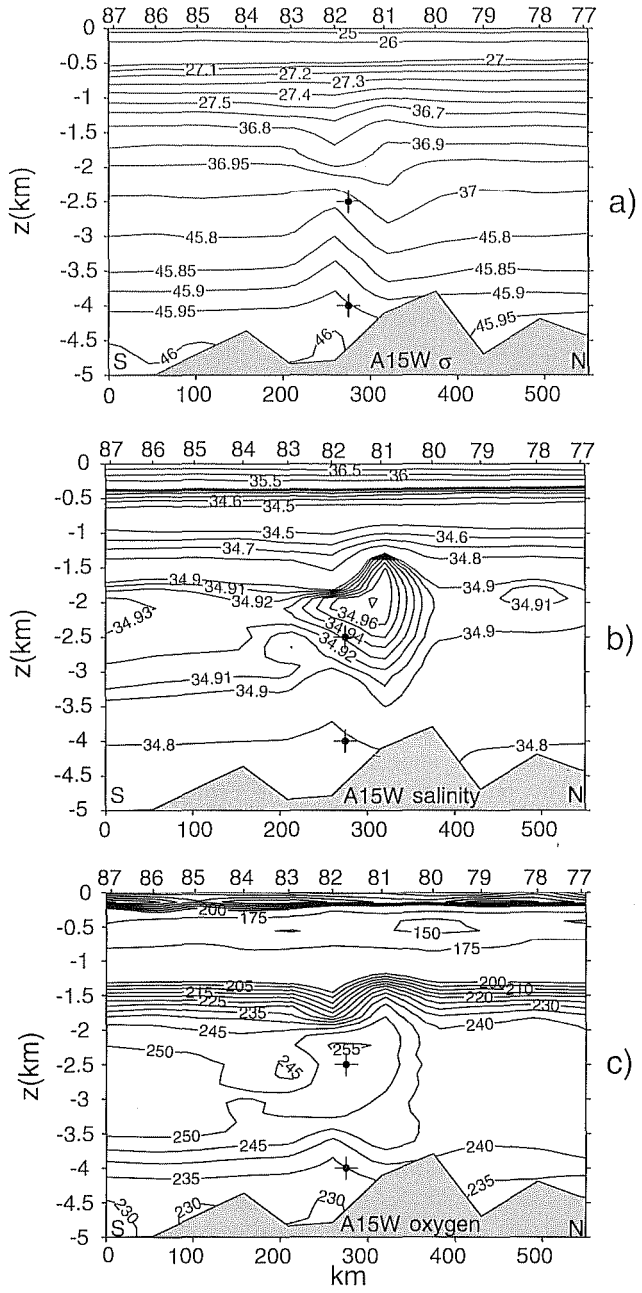

Figure 5. Like Figure 3 except for the A15W stations 77–87. A ceddy-like feature is at station 82, with its core at ≈2300 m depth, and an aeddy-like one is at station 81, with its core at ≈1800 m depth. S and N in the bottom corners denote south and north. The dotted cross-like symbols are the locations of two deep floats.

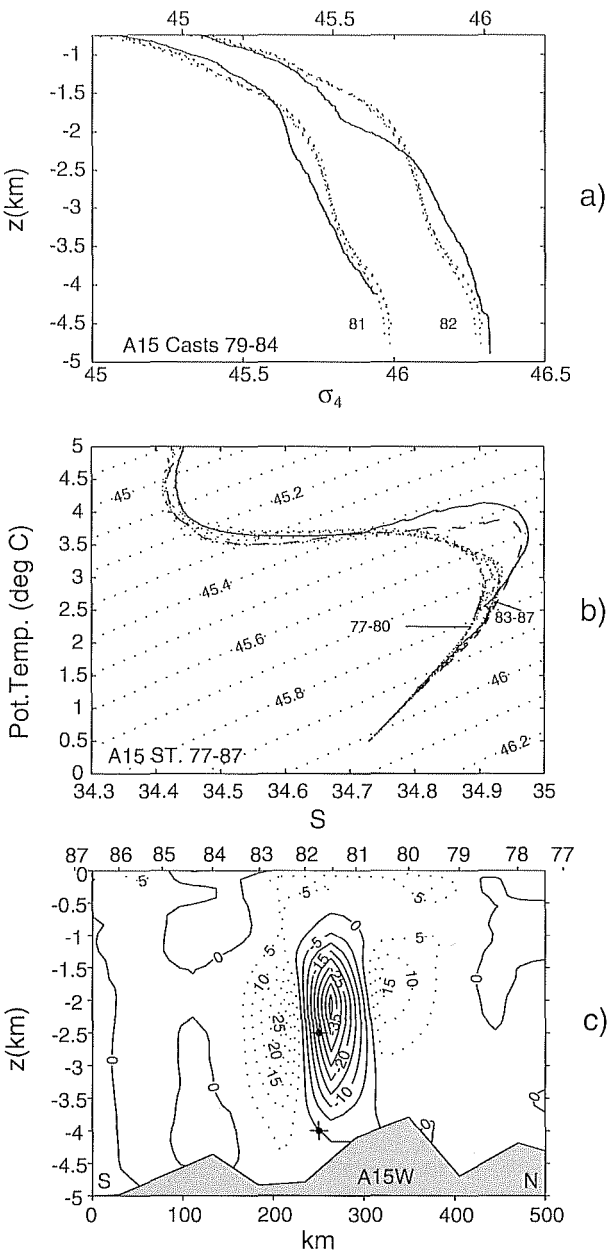

Figure 6. (a) The σ_4 versus depth for A15W: (left curves) stations 79–81 and 83–84 (with the abscissa on the bottom) with station 81's values the solid line and (right curves) stations 79–80 and 82–84 (with abscissa on the top) with station 82's values the solid line. The aeddy-like feature (as in Figure 5a) at station 81 has its core at about 1800 m depth and extends upward and downward to about 800 m depth and 3300 m depth, respectively, and the ceddy-like feature at station 82 has its core at 2300 m depth and extends upward to about 1600 m depth and downward to about 4000 m depth. Figure 6a allows depths to be determined in Figure 6b. (b) The θ-*S* plots for the stations shown in Figure 5 with stations 81 and 82 values the solid and dashed lines, respectively. The σ_4 contours are shown. (c) Geostrophic velocity section for A15W stations 77–87. Values are in cm s^{-1}, and positive values are into the plane of the figure. The level of no motion is at the bottom. The dotted crosses denote positions of two deep floats launched during A15W (see text). S and N in the bottom corners denote south and north.

is an O_2 core but not a *S* core, and at station 81 there is a *S* core but not an O_2 one; otherwise, the former and latter resemble an eddy and an aeddy, respectively, in terms of density and anomalous θ-*S* properties. To see if we might get a better, or perhaps a different, insight in what we sampled, we redid Figures 5a–5c and Figure 6c inserting different data midway between stations 81 and 82. This was done to simulate what might have been inferred if an additional station had been made between these two stations and if that station had properties resembling (1) those of

station 81, (2) those of station 82, (3) those of a station outside of the feature and to the north of the front at which it is found, and (4) those of a station outside of the feature and to the south of the front at which it was found. To simulate cases 1, 2, 3, and 4, we inserted data from A15W stations 81, 82, 77, and 87, respectively. For cases 1 and 2 we found qualitatively what is seen in Figures 5a –5c and Figure 6c. Thus, again, in terms of density a ceddy-like feature is seen to the south and an aeddy-like feature is seen to the north, there is a single, pear-shaped S core determined by station 81 and a single O_2 core determined by station 82, and the velocity section is essentially the same except where the eddies reinforce, the speed now doubles. Case 3 qualitatively resembles what is seen in Figures 5a–5c and Figure 6 except that now there are two S cores, one at station 81 and the other at station 82. Case 4, reproduced in Appendix A, also resembles what is seen in Figures 5a–5c and Figure 6 except that stations 81 and 82 each have a S and an O_2 core. We suspect that the feature that was sampled was a ceddy and aeddy in contact and that just as they came in contact, they looked like Figure A1 in Appendix A.

3. What Was Seen on A15S

[15] The A15S section, which was planned to be approximately along 18°S beginning at and going to the west of 19°W, began about 10 days later, after the taking of A15W stations 81 and 82. In an attempt to revisit whatever had been sampled, two additional stations were added to the north and east of the previously planned start location of A15S, 19°S, 19°W. The first revised station was 110 (2017–2336 UTC; 8 May 1994; 18°37′S, 17°54′W), which was about 110 km to the east of the A15W station 82, and the second was 111 (0418–0718 UTC; 9 May 1994; 18°42′S, 18°28′W), which was halfway between the revised 110 and A15W station 82 (Figure 1 insert). Further, the previously planned first A15S station at 19°W was shifted to be about 50 km to north, at A15W station 82, to become the third station along A15S, station 112 (1030–1319 UTC; 9 May 1994; 18°19.0′S, 19°0′W). (A15S then proceeded, roughly as originally planned, at station 113 (1819–2132 UTC; 9 May 1994; 19°0′S, 19°32′W)). The expectation was that whatever it was, it was likely to be moving toward the west. From Figures 2c and 7 it is apparent that the expectation of net westward motion, if indeed what was observed at A15S stations 110 and 112 was what was seen at A15W stations 81 and 82, was not met; one unusual feature was seen on A15W (at station 82), and the other is 110 km farther to the east. We argue below that what was seen on A15S was perhaps the features seen on A15W after being altered by their interaction and a new feature resulting from their collision.

[16] Three cores are suggested in Figures 7b and 7c rather than the one suggested for A15W in Figures 5b and 5c (or the two seen in the doctored A15W section Figures A1b and A1c. Two cores, one on top of the other, appear to exist at station 110 (their eastern edges are not delineated because of the limited sampling to the east): one between 1400 m $\leq$ depths $\leq$ 2500 m for S (1900 m $\leq$ depths $\leq$ 2400 m for O_2) and the other between 2600 m $\leq$ depths $\leq$ 3300 m for S (2700 m $\leq$ depths $\leq$ 3400 m for O_2) (Figures 7b and 7c). A core is seen at station 112 at 1500 m $\leq$ depths $\leq$ 2300 m for S (1800 m $\leq$ depths $\leq$ 2300 m for O_2) (Figures 7b and 7c).

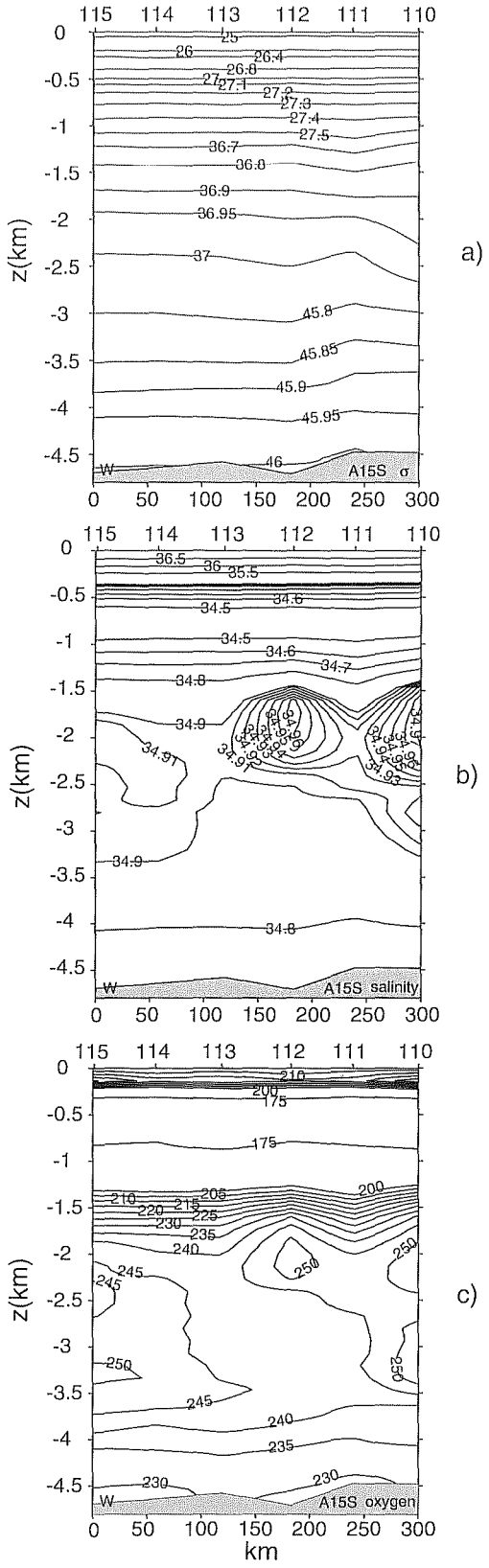

Figure 7. Like Figure 3 except for the A15S section. W in the bottom left corner denotes west. The features at stations 110 and 112 are in contact at station 111. (a) The lowest density surface is σ_4 = 46.00. (b) and (c) A single-core structure is seen at station 112 and a double-core structure, one on top of the other, is seen at station 110.

[17] S and O_2 profiles at station 110 (not shown) indicate that the two S and O_2 cores shown at this station in Figures 7b and 7c are likely real and are not an artifact of contouring data at the end of a section. This is further substantiated by Θ-S and density-depth plots for this station (Figures 8a and 8b), which show that the unusual, relatively cool and fresh water between $45.70 < \sigma_4 \leq 45.75$ (Figure 8c) is found at 2425 m $\leq$ depths $\leq$ 2680 m, which corresponds to water between the two cores shown in Figures 7b and 7c. In terms of θ-S properties the two cores at station 110 appear to have different source regions. Those of the upper core at A15S station 110 are essentially the same as those seen in the bolus of the aeddy at station 81 in the A15W section for $45.43 \leq \sigma_4 \leq 45.70$ (Figure 8a). This range of σ_4 corresponds to 1220 m $\leq$ depths $\leq$ 2425 m at A15S station 110 (Figure 8b) and to 1160 m $\leq$ depths $\leq$ 2500 m at A15W station 81 (Figure 6a). For $45.43 \leq \sigma_4 \leq 45.48$ (1220 m $\leq$ depths to 1360 m) (Figures 8a and 8b) the upper bolus's θ-S properties appear like those of the A15 W station 81 eddy modified by interleaving with a less salty, cooler water type, like that of the ceddy at A15W station 82. The θ-S properties of this lower core correspond to those of the ceddy at A15W station 82 for $45.75 \leq \sigma_4 \leq 45.87$ (Figure 8c). This corresponds to 2680 m $\leq$ depths $\leq$ 3435 m at station 110 (Figure 8b) and to 2330 m $\leq$ depths $\leq$ 3165 m for A15W station 82.

[18] The θ-S properties associated with the core at A15S station 112 are consistent with interleaving of the boluses at A15W stations 81 and 82 for $45.40 \leq \sigma_4 \leq 45.71$ (1140 m $\leq$ depths $\leq$ 2240 m) (Figures 8b and 8d). This corresponds to 1090 m $\leq$ depths $\leq$ 2545 m for A15W station 81 and 1320 m $\leq$ depths $\leq$ 2225 m for A15W station 82 (Figure 6a).

[19] The above θ-S properties at A15S station 110 suggest that the upper bolus there could be a part of the A15W station 81 aeddy and that the lower bolus could be a part of the A15W station 82 ceddy. However, the inferred geostrophic velocity field with the LNM at the bottom is consistent only with the upper bolus' being part (half) of an eddy centered at station 110 (Figure 9a). It is not consistent with the lower bolus' being part (half) of an aeddy centered at station 110; rather, this bolus appears to be part of the aeddy above it (Figure 9a). What is seen at A15S station 112 in Figure 9a suggests that the interleaving of the water from A15W stations 81 and 82, if indeed that did occur and if that interleaved water is what is seen at A15S station 112, resulted in a weak eddy with a maximum swirl speed of $\approx$3 cm s^{-1}.

[20] The features at A15S stations 110 and 112 are in contact at station 111 (Figures 7b and 7c). Also, Figure 8b (left curve) indicates that station 110's density structure is aeddy-over-ceddy-like when compared to the density of neighboring stations not in the features. We thus replaced station 111's data with those from a neighboring station not in those features (in this case, station 115) to simulate what the flow field would be like if the features at stations 110 and 112 were not in contact. The resulting, partially simulated, flow field qualitatively does not change for the upper core at station 110 and the core at station 112, but it does change sign for the lower core at station 110 (Figure 9b). The flow field is then consistent with the previous inference, from θ-S properties, that the lower core at A15S station 110 appears to be part of the remnant of the A15W station 82 ceddy.

4. Origin of the A17 and A15W Ceddies and the A15W Aeddy

[21] We attempt in this section to infer where the anomalous water seen in the A17 and A15W ceddies and the A15W aeddy may have originated. As previously noted, the anomalous water is found in NADW and is relatively saltier and warmer on isopycnals compared to surrounding water.

[22] Any eddy formed from the pinching off of a meander on the offshore side of the Deep Western Boundary Current (DWBC) of NADW would likely be cyclonic. Thus the seaward side of the DWBC of NADW appears a likely source region for the ceddies. However, instabilities of the DWBC should not lead to the exclusive formation of ceddies if one refers to observations in other basins. For example, some anticyclonic Gulf Stream eddies have been observed on the offshore side of the Gulf Stream and have been attributed to interactions of this current with seamounts [*Richardson*, 1980; *Brundage and Dugan*, 1983] or to instabilities on outbreaks on the seaward side of the Gulf Stream [e.g., *Cornillon et al.*, 1986]. In the eastern North Atlantic a simultaneous detachment of Meddies and cyclones from the Mediterranean Undercurrent is sometimes observed [*Serra and Ambar*, 2002], and in the Mediterranean Sea, pairs of opposite-signed vortices also form at instabilities of the Algerian Current [*Millot*, 1991]. Thus the western portion or edge of the DWBC of NADW also appears to be a likely source for the A15W station 81 aeddy.

4.1. A17 Ceddy

[23] We consider θ-S curves in the vicinity of the eastern edge of the DWBC of NADW in the following zonal or quasi-zonal sections: WOCE A9 (19°S), Oceanus 133 (24°S), SAVE3 (~25°S), WOCE A23 (~27°S), and WOCE A10 (30°S) (Figure 1). The tilde here denotes the approximate latitude of stations on the eastern edge of the DWBC on quasi-zonal sections, and we recall that the A17 ceddy was at 26°S. For SAVE3, WOCE A23, and WOCE A10 the θ-S curves transition from being too salty and warm in the DWBC to being too fresh and cool on the seaward side of the DWBC relative to the A17 ceddy (e.g., Figure 10a). While no complete match of θ-S curves was seen, the A17 ceddy θ-S curve is "sandwiched" between θ-S curves on the seaward side of the DWBC and those in the DWBC on these sections, and the sandwiching is better for the A10 and A23 sections than for SAVE3. Farther to the north this sandwiching behavior is absent as the A17 ceddy water there is always fresher and cooler relative to the waters in and on the seaward edge of the DWBC (not shown). We conclude this ceddy was likely formed on the offshore side of the DWBC of NADW in the latitude range 27°–30°S and thus $\approx$400 km westward from where it was observed.

4.2. A15W Ceddy

[24] Similarly to the A17 ceddy, we consider θ-S curves but for the following sections: A7 (4.5°S), A8 (11°S), A17 (13°S), A15S (18°S), WOCE A9 (19°S), and Oceanus 133 (24°S) (Figure 1). The only two sections where the A15W station 82 θ-S was sandwiched between θ-S curves on the seaward side of the DWBC and those in the DWBC were A15S and A9 (e.g., Figure 10b). We conclude that this ceddy may have been formed in the latitude range 18°–19°S about 2100 km west of where it was observed.

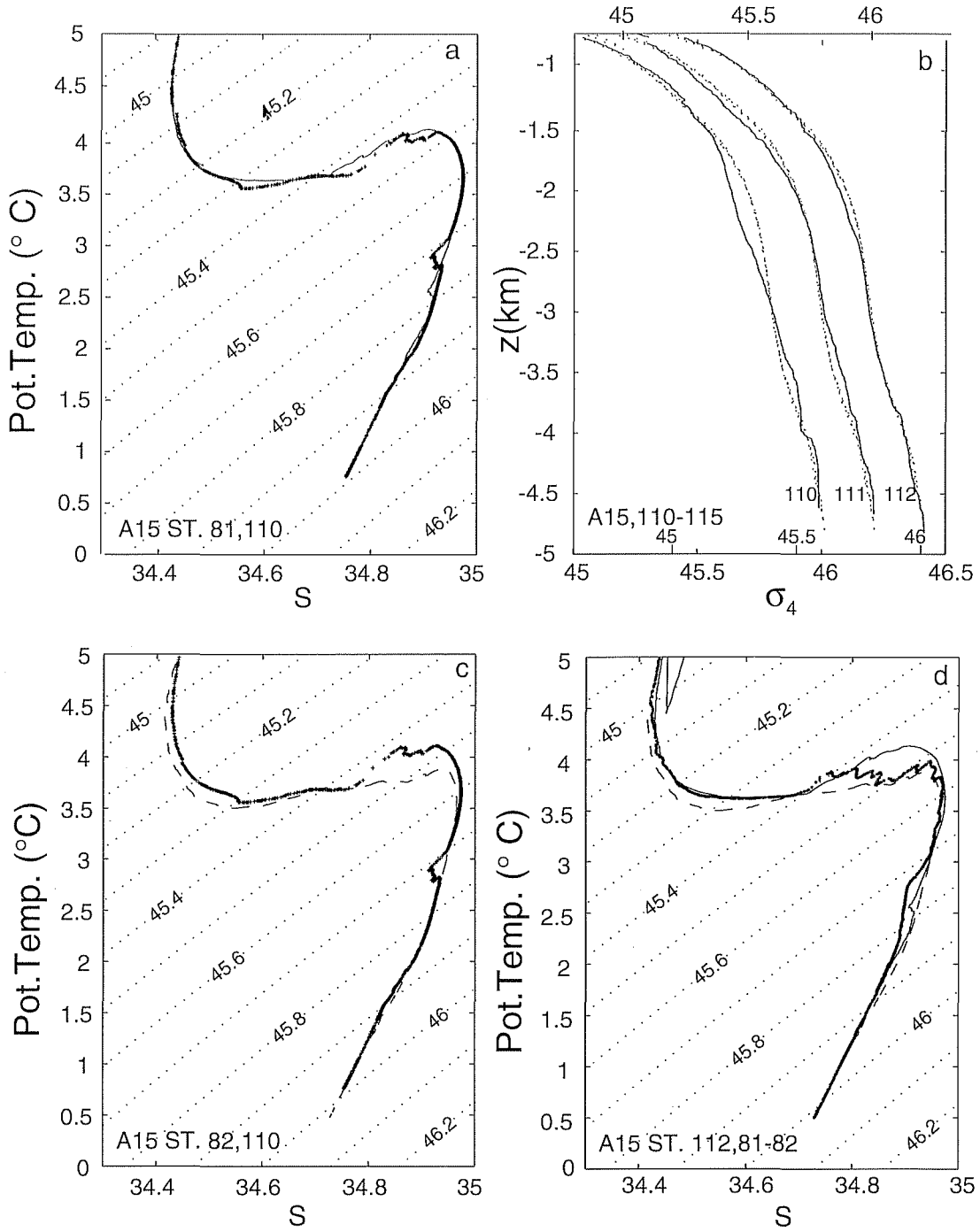

Figure 8. (a) The θ-*S* plots for station 81 (thick crosses) in the A15W aeddy and station 110 (solid line) in the A15S section. The σ_4 contours are shown. The curves basically overlay for $45.43 < \sigma_4 < 45.70$ with some interleaving indicated for $45.44 < \sigma_4 < 45.48$ in station 110's values (see text). (b) The σ_4 versus depth for (left curve) stations 110 (solid line) and 113–115 (dotted lines), with abscissa at bottom lower; (center curve) stations 111 (solid line) and 113–115 (dotted lines), with abscissa at top; and (right curve) stations 112 (solid line) and 113–115 (dotted lines), with abscissa at bottom upper. Relative to stations 113–115 (i.e., neighboring water) station 110's σ_4 profile is consistent with a portion of an aeddy centered at ≈1400 m depth being over a portion of an aeddy centered at ≈3000 m depth(see text). Station 111's σ_4 profile is consistent with a ceddy, but because there is no bolus, no ceddy is inferred. Station 112's σ_4 profile is consistent with a weak aeddy centered at ≈1400 m depth (barely evident in its upper half). (c) The θ-*S* plots for A15W stations 82 (dashed line) and 110 (thick crosses); σ_4 contours are shown. The curves basically overlay for $45.75 < \sigma_4 < 45.87$ (see text). (d) The θ-*S* plot of station 112 (thick dots) with those of A15W stations 81 (solid line) and 82 (dashed line) overlain. For $45.40 < \sigma_4 < 45.71$, station 112's values indicate interleaving between stations 81 and 82's waters (see text).

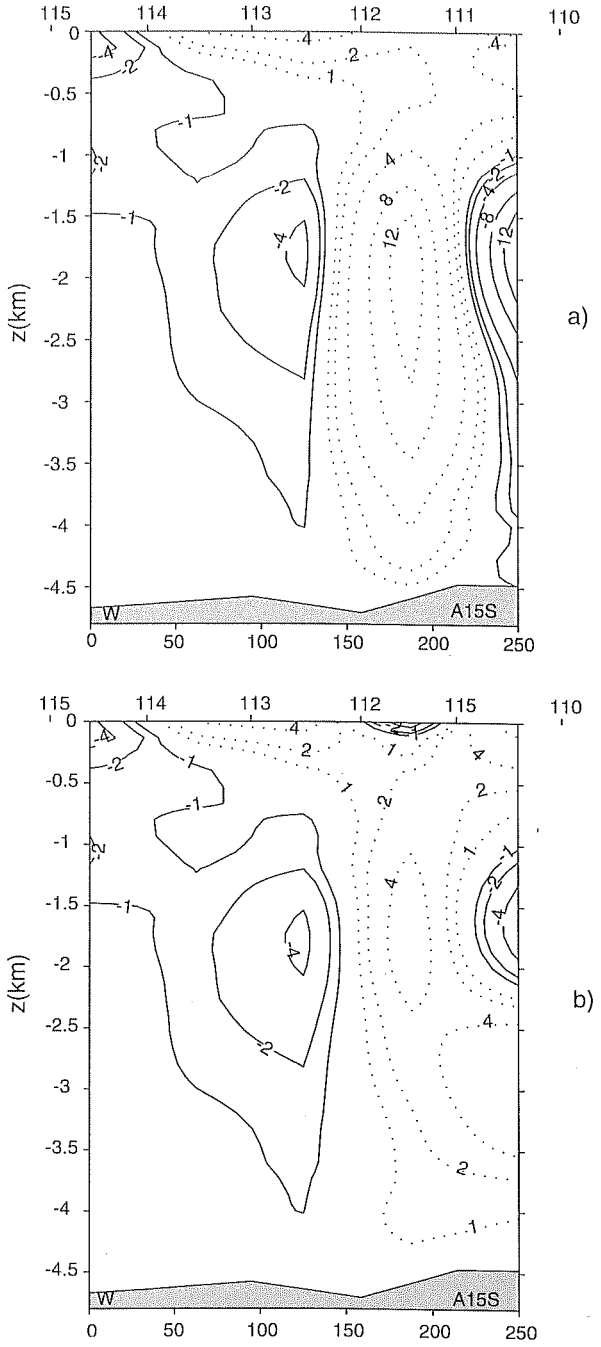

Figure 9. (a) Geostrophic velocity section for A15S stations 110–115 with the LNM at the bottom. Values are in cm s^{-1}, and positive values are into the plane of the figure. Contour interval is in multiples of 4 cm s^{-1}, except the zero contour is omitted and the ±1 and ±2 cm s^{-1} contours are added. The flow pattern is consistent with an aeddy centered at station 112, with its core at ≈1800 m depth, and a part of an aeddy at station 110, with its core at ≈1800 m depth. However, there is no indication of a part of a ceddy below the aeddy at station 110 (see text). W in the lower left corner denotes west. (b) A doctored version of Figure 9a with a surrounding station, here station 115, replacing station 111 (see text). The resulting flow pattern suggests, consistent with Figures 8a and 8b (left curve), that the lower core at station 110 may be a portion of a ceddy (see text) and the same contouring interval as in Figure 9a.

4.3. A15W Aeddy

[25] That the bolus of this aeddy has saltier, warmer NADW characteristics than the bolus of the A15W ceddy suggests it may have been formed to the north of where the A15W ceddy was formed. We compared the θ-*S* curve of this æddy to the sections A7 (4.5°S), A8 (11°S), and A17 (13°S) and concluded that the upper part of this aeddy's bolus, 1200 m ≥ depths ≥ 2500 m, could have originated in the DWBC of NADW in the latitude range 11°–13°S (Figure 10c, $45.42 \leq \sigma_4 \leq 45.70$) about 2500 km to the west-northwest. We further conclude that the lower part of this bolus, 2500 m ≥ depths ≥ 3700 m, is just local surrounding water found to the south of the θ-*S* front in NADW previously noted (where the A15W feature was found). That this aeddy could have been formed from the interaction of the DWBC with a seamount, in this region, is possible because of the presence of the Bahia Seamounts there (see Figure 1).

[26] Another possible source region is an extensive tongue extending seaward from the western boundary at ≈10°S, which is evident on *S* on the density surface $\sigma_2 = 36.98$ (Figure 11). This density surface is at about 1700 m depth in the Brazil Basin, which is also the approximate depth of the core of the A15W aeddies. If this tongue is due to a seaward extrusion or squirt of the DWBC of NADW, then an eddy shed from it could be an aeddy. Some stations from A17 that cross the southern side of this extrusion along 31°W have θ-*S* properties consistent with the A15W aeddy's having been formed there (Figure 12). However, θ-*S* properties of stations crossing the extrusion farther to the east, along 25°W, (not shown) do not. The 25°W section was made in the 1980s, while most of the sections considered here are WOCE sections made in the 1990s. The question of decadal variability of NADW in the Brazil Basin is not addressed in this study; thus whether the above differences are due to regional or temporal variability is unknown. However, we have noticed nothing exceptional about NADW properties in the two other 1980s pre-WOCE sections considered here (SAVE3 and OCC 133-24S).

4.4. DWBC Extrusions As Ceddy Source Regions

[27] In section 4.3 we mentioned that one possible source region for the A15W aeddy was an extrusion extending seaward from the DWBC at about 10°S. This suggests considering whether this extrusion and two other similar protrusions seen in Figure 11 near 31° and 21°S are possible source regions for ceddies. The θ-*S* properties of A17 stations spanning the protrusions (not shown), however, are not consistent with the A17 and A15W ceddies' being formed there.

[28] During the A15 cruise one of us (G. W.) thought that what was seen at stations 81 and 82 might have been formed to the northeast at the equator (a salty, narrow tongue at the equator is indicated in Figure 11). However, later we concluded that because the NADW θ-*S* properties of A15W stations at the equator were too cool and fresh, this could not have been the source region. We also concluded from θ-*S* properties that the lower portions of the features could have been formed farther to the west along the equator between 25°W (SAVE6) and 19°W

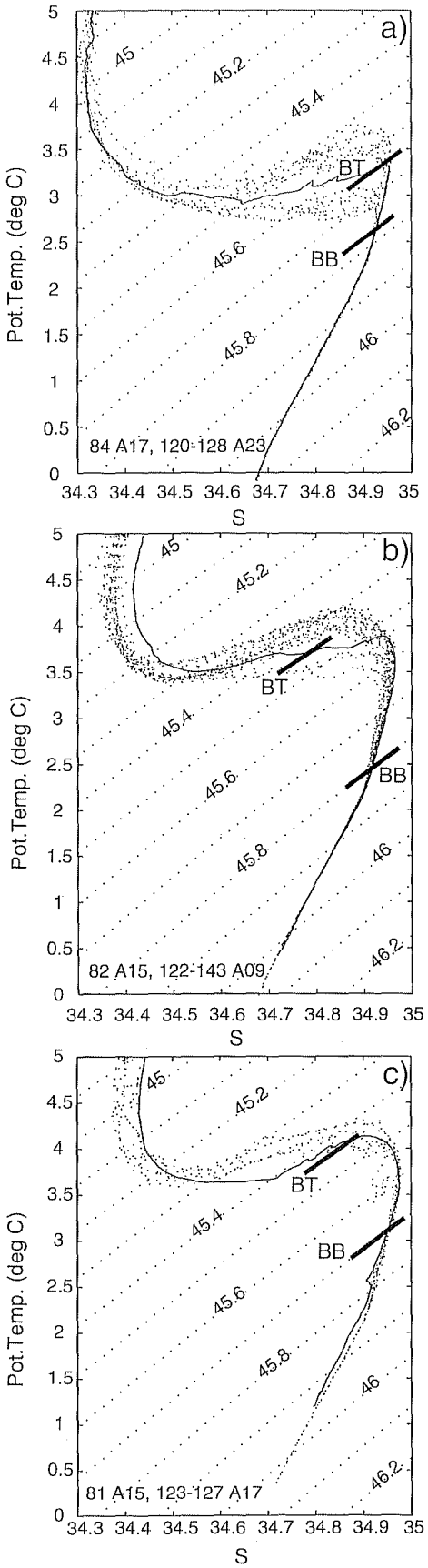

(A15W) (not shown), but this is unlikely as only a relatively thin portion of the boluses could be so accounted.

5. Summary and Discussion

[29] We have reported observations in the Brazil Basin of what we think were deep submesoscale eddies. These were detected during two WOCE hydrographic surveys, A15 and A17, where the station spacing 55 km was comparable to the internal Rossby radii of deformation. Only one cast was made in each eddy. Presuming they were approximately circular and that they were indeed eddies, we conclude that these eddies' diameters are smaller than 110 km and that their maxima swirl speeds exceed 14 cm s^{-1} for the A17 station 84 ceddy (cyclonic eddy), 27 cm s^{-1} for the A15W station 82 ceddy, 17 cm s^{-1} for the A15W station 81 aeddies (anticyclonic eddy), and 3 cm s^{-1} for the A15S station 112 aeddies. The A15W station 81 aeddy, except for its vorticity, was similar in size, depth range, and swirl speeds to the two ceddies. The A15S station 112 aeddy was similar to the A15W station 81 one except that its swirl speeds were much weaker. As described here, the two ceddies are similar in dimension, swirl speed, and depth at which they were centered to those described for the North Atlantic from hydrographic and moored current meter measurements by *Colin de Verdière et al.* [1989] and *Schauer* [1989]. Float measurements in the Brazil Basin in ceddies at 1800 [*Richardson and Fratantoni*, 1999] and 2500 m depth [*Hogg and Owens*, 1999] had generally smaller swirl diameters of 30–60 km. This suggests that we may have overestimated the deep eddies' diameters by a factor of about 2 and correspondingly underestimated their swirl speeds.

[30] We think it likely that the A15W station 82 and the A17 station 84 ceddies were formed from ejections of the DWBC of NADW; *Richardson and Fratantoni* [1999] concluded the same thing for the ceddy they saw in the northwestern Brazil Basin. Our ceddies' anomalous θ-S properties were consistent with their being formed at the seaward edge of this DWBC: between 27° and 30°S for the A17 one and between 18° and 19°S for the A15W one. We also concluded that the A15W station 81 aeddy was also likely formed in the western basin near or in the DWBC between 11°–13°S. Being from the DWBC implies that the A17W station 84 and A15W station 82 eddies and the A15W station 81 aeddy had moved to the east after formation. The ceddy in Figure 8 of *Richardson and Fratantoni* [1999] first moved eastward for about 3 months, then westward for about the same time period. The movement of the ceddy seen in Figure 8a of *Hogg and Owens* [1999] is discussed below.

Figure 10. (opposite) The θ-S plots for (a) A17 station 84 (thicker symbol) with those for A23 (dots) in and just to the east of the DWBC of NADW, (b) A15W ceddy station 82 (thicker symbol) with those for A9 (dots) in and just to the east of the DWBC of NADW, and (c) A15W station 81 (thicker symbol) with those for A17-13S (dots) in and just to the east of the DWBC of NADW. BT and BB denote the top and bottom of the boluses. Here σ_4 is contoured.

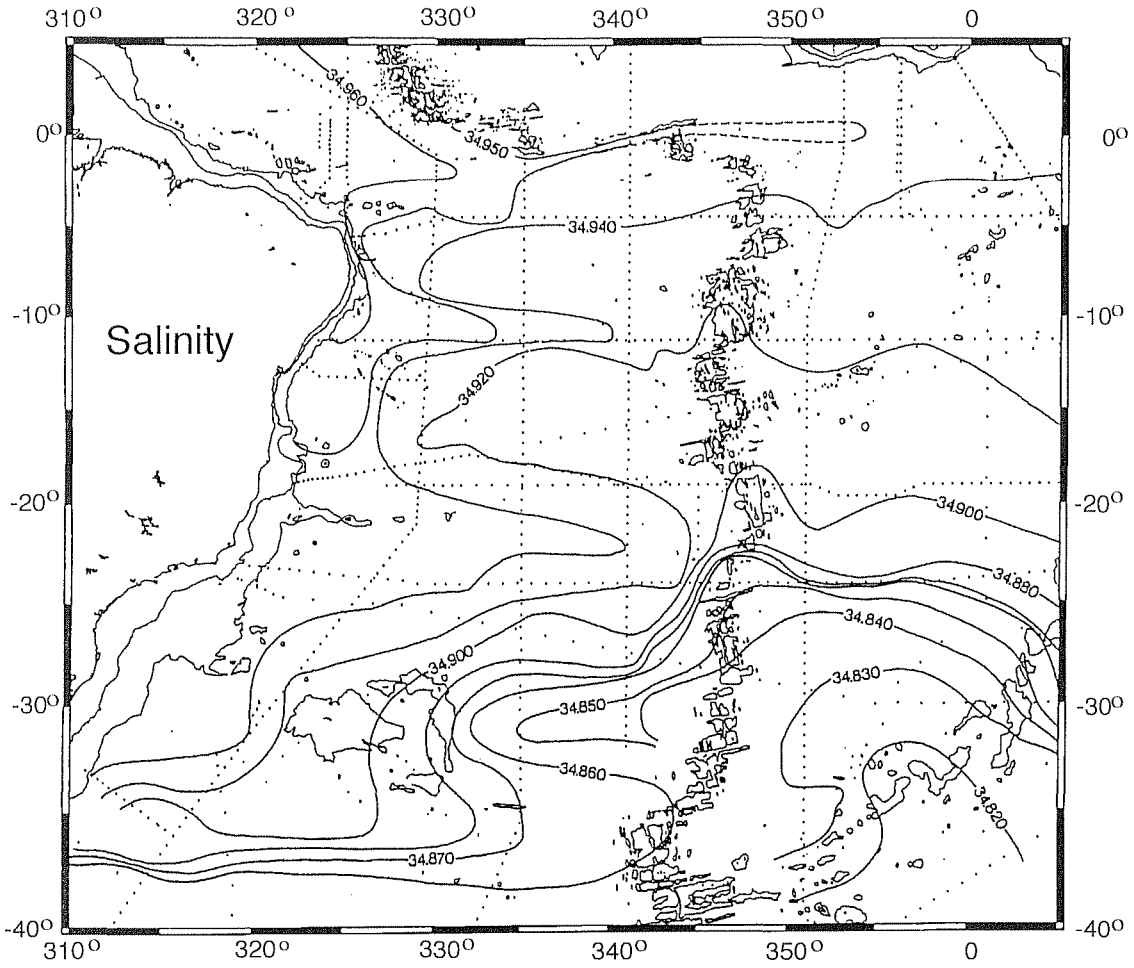

Figure 11. Hand-drawn salinity on $\sigma_2 = 36.98$; data are at the dots. This density surface is at about 1700 m depth, which is the approximate depth of the core of the A15W station 81 eddy. The 200 and 3000 m depth contours are shown.

[31] The unusual features seen at stations 110 and 112 on A15S had θ-S properties consistent with their being either the remnants of or a combination of the same unusual features seen at stations 81 and 82 about 10 days earlier on A15W. Two features at station 110 were consistent with the upper being the remnant of the station 81 eddy and the lower being the remnant of the station 82 ceddy, and the feature at station 112 appeared to be a combination of some of the features at stations 81 and 82. However, the inferred geostrophic velocity field (Figure 9a) only partially supported this. We think it unlikely that what may have been part of a ceddy at A15W station 82 could 10 days later be observed at A15S station 110 as part of an aeddy, which would follow from Figure 9a and our θ-S interpretation (Figure 8). Perhaps what was seen at A15S stations 110 and 112 is not attributable to features sampled during A15W. We think it noteworthy, arguing against that possibility, that of all the many reported deep hydrographic stations made in the Brazil Basin (the associated sections of many of these are shown in Figure 1), only five, those reported here, have shown what appears to be deep eddies and that four of these were within $\approx$110 km of each other and were taken in the same $\approx$10 day period. Thus we attempted to seek an explanation for the features seen on A15S in terms of the features seen on A15W.

[32] The apparent contradiction between the velocity field and the θ-S properties in the lower part of the station 110 feature might result from an insufficient lateral resolution and the ensuing failure to sample the exact boundary between the features of stations 110 and 112. Supporting this is that station 110's density structure suggests an aeddy over a ceddy when compared to neighboring stations not in eddies (Figure 8b). With A15S station 111 replaced by another station not in contact with the features (here taken as station 115) the resulting velocity field (Figure 9b) was in agreement with the θ-S properties interpretation. If correct, the aeddy at A15W station 81 would had traveled at $\approx$15 cm s^{-1} toward the east-southeast to be part of what was seen at A15S station 110. Similarly, the ceddy at A15S station 82 would have traveled toward the east at $\approx$14 cm s^{-1} to become part of what was seen at A15S station 110.

[33] Two floats, one set for 2500 m depth and the other for 4000 m depth, were launched during A15W at 1929 and 1923 UTC, respectively; 28 April 1994; 18°34.5′S, 19°0.0′W between the taking of stations 81 and 82. Their positions at intended drift depths are given in Figures 5b, 5c, 6c, and 14a–

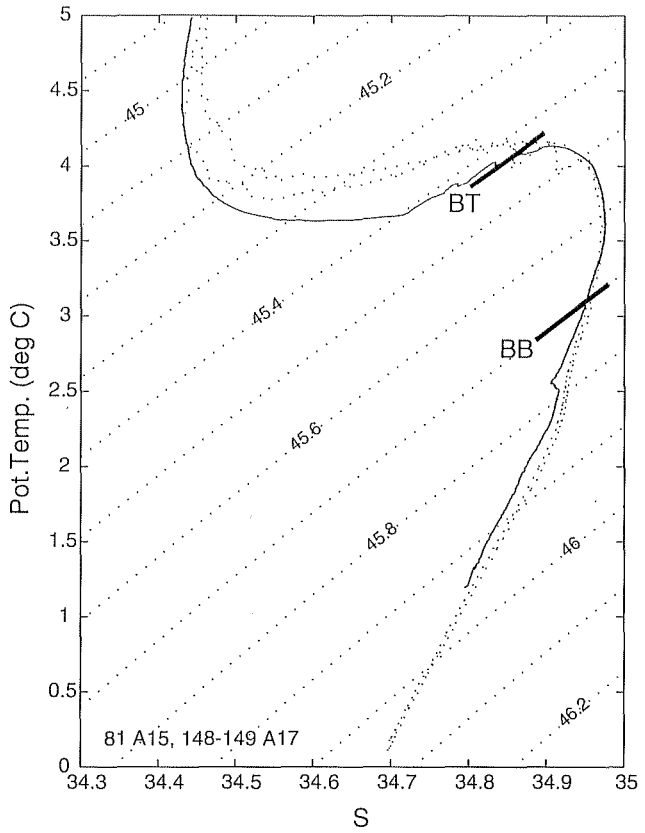

Figure 12. The θ-*S* plots for A15W station 81 (thicker symbol) with those for A17 stations 148–149 (dots) at 10.5°S, 30.4°W and 10.0°S, 30.4°W, respectively. BT and BB denote the top and bottom of the eddy bolus. Here σ_4 is contoured.

14d. After 10 days the 2500 m float had moved to the east-southeast at an average speed 14 cm s^{-1}, and the 4000 m float had moved to the northeast at 4 cm s^{-1} (N. G. Hogg, personal communication, 2001). (Ranging uncertainties for the first 2 weeks are such that it is unknown whether the 2500 m float executed cyclonic movement then (N. G. Hogg, personal communication, 2001). Afterward, it appeared to move in a ceddy that was stalled for a few weeks, which then moved to the south and then to the southwest [*Hogg and Owens*, 1999, Figure 8a].) The position of the 2500 m float after launch appears to be in the lower limits of the bolus of the A15W station 82 ceddy (Figures 5b and 5c), and its net drift rate is consistent with the lower bolus seen at A15S station 110 being part of the bolus water seen 10 days earlier at A15W station 82. We would not expect ceddy water that is not part of its bolus to follow the bolus, and hence the slow drift to the northeast of the float at 4000 m depth seems reasonable.

[34] The implied above ≈14–15 cm s^{-1} eddy drift rates are about 5 times larger than the averaged motions of the best studied deep eddies, Meddies, and are directed toward the east rather than toward the west. The large drift rate could be due to self-advection of the two coupled vorticies. The only example of a deep, coupled translations rate we are aware of is an estimate of 8.1 cm s^{-1} during the interaction between two Meddies [*Schultz-Tokos et al.*, 1994]. Though lower than our value, it shows that significant accelerations of an eddy motion can occur during phases of mutual advection with another structure. Another possibility for the large translation rate is advection by the eastward flow associated with the Namib Col Current [*Speer et al.*, 1995], seen as the salty tongue between 20° and 25°S in Figure 11, if this current extends as far north as 18°S. While we are unaware of any observed deep eddy/strong current advection rates, cold-core rings interacting with the Gulf Stream were shown to move with velocities up to 25 cm s^{-1} [*The Ring Group*, 1981]. However, for reasons presented below (i.e., a third eddy in the region may not have moved much) we think the self-advection explanation more likely.

[35] Reasons for thinking that the A15S station 112 aeddy may have resulted from the interaction of the A15W station 81 aeddies and the station 82 ceddy were that its bolus has θ-*S* properties intermediate to their boluses, that its θ-*S* plot indicated interleaving, and that it was observed at the repeat of A15W station 82. On the basis only of these bolus property arguments we suggest below a scenario for the deep eddy interaction. We are conscious that a dynamical interpretation would be required to validate it, but we have not been able to find any theoretical (nor laboratory or observational) basis to support or counter it. Hopefully, the following interpretation may stimulate more interest in how deep eddies of opposite vorticity interact after they come into contact.

[36] The process that we think may have occurred is sketched in Figure 13. Figure 13a depicts the case just before the eddies come into contact (at or just before the time the features were seen in A15W). The situation is simplified to be a four-density fluid with the density of the core of the (station 82) ceddy, ρ and the density of the core of the (station 81) aeddy, ρ′ (Figure 13a). It seems plausible after contact had been made (Figure 13b) that since $\rho' > \rho - \Delta\rho$, some of the upper portion of the aeddy would have spilled into the region just above the ceddy with, in turn, the ceddy beginning to move to be under the aeddy to replace some of the spilled fluid. Some interleaving of the upper aeddy water with that which had been above the ceddy is shown as the hatched fluid region in Figure 13b. In Figure 13c the region that originally had been immediately above the ceddy is shown to be water of density $\rho - \Delta\rho$ interleaved with water of density ρ. Since this region is composed of waters initially with zero vorticity (those immediately above the ceddy in Figure 13a) with that of negative vorticity (that of the upper aeddy in Figure 13a), the resulting feature is expected to have some negative vorticity (i.e., it is expected to be a weaker eddy than that of Figure 13a). Further, it would have an average density intermediate to $\rho - \Delta\rho$ and ρ′. The water in the new aeddy is shown as interleaved, as the ≈10 days between Figures 13a and 13c is probably too short for effective mixing of the two water types. The ceddy, shown moving toward the original aeddy to replace spilled fluid in Figure 13b is now below it in Figure 13c. Figure 13c appears to agree with the observed anomalous water properties (Figure 8) and in part with the inferred geostrophic velocities (Figure 9a). A difficulty in comparing our observations with previous theoretical results comes from our poor sampling of the features. Laterally, the large uncertainty of the eddy scales

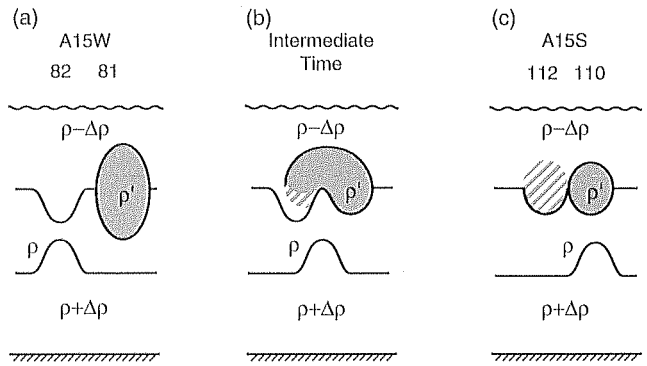

Figure 13. Cartoon of what may happen if a ceddy and an aeddy collide as proposed in the text. (a) The density of the ceddy (at station 82) is ρ and that of the aeddy (at station 81) is ρ' with $\rho' < \rho$. Both are surrounded on the top with fluid of lighter density $\rho - \Delta\rho$. The aeddy is surrounded below with fluid of density ρ, and the ceddy is surrounded below with fluid of density $\rho + \Delta\rho$ with $\rho + \Delta\rho < \rho$. What is represented is just before the ceddy and aeddy come into contact. The cores are to be associated with the NADW DWBC component waters of both abyssal eddies. (b) An intermediate time between A15W and A15S during the collision. (c) The time of the A15S section (about 10 days after Figure 13a). In Figure 13b some of the aeddy's water spills into the upper portion of the ceddy and interleaves with the fluid there. The lower portion of the ceddy begins to move toward the aeddy (perhaps to replace some of the water that spilled over). In Figure 13c, what was once the upper portion of the ceddy is now a new aeddy (the stippled region) at station 112 composed of water of density ρ' interleaved with water of density $\rho - \Delta\rho$ whose average density is intermediated to ρ' and $\rho - \Delta\rho$. The lower part of the ceddy is shown as being now under the original, somewhat thinner aeddy at station 110.

(the station spacing of 55 km is only a maximum scale) impedes dynamical interpretation as the way eddies interact is often dependent on their sizes. For instance, *Polvani* [1991] pointed out that two vortices in different layers of a two-layer fluid will possibly coalesce only if their radii are comparable to, or larger than, the Rossby deformation radius. With a first internal deformation radius comparable to the upper limit of the eddy radii the apparently observed subsequent vertical alignment of the A15W station 82 ceddy with the A15W station 81 aeddy cannot be supported nor discarded.

[37] Regarding the temporal evolution of the structures, we cannot say, from only two samplings at a 10 day interval, how long the A15W ceddy and aeddy may have been coupled together before being sampled nor whether the situation represented in Figure 13c is a stable one or not. If, indeed, what was seen at A15W stations 81 and 82 were an aeddy and a ceddy in contact and if they were formed at or near the DWBC of NADW, we do not think that these features were formed together and traveled from their formation region as a coupled pair to where they were observed. As noted in section 4, we thought it likely that one had been formed around 11°–13°S, and the other around had been formed around 18°–19°S. Further, our proposed account of what may have happened after they collided (Figures 13b and 13c) suggests that paired cyclonic-anticyclonic eddies with slightly different core densities do not readily travel coupled side by side for long periods. We suspect that before they interacted they had translational speeds of about 3 cm s^{-1} on the basis of the observations of *Richardson and Fratantoni* [1999] and that they could not have been in contact for long before we observed them. If correct, this would imply that the A17 station 84 ceddy was a few months old and the A15W stations 81 and 82 deep eddies were order a year or so old provided they originated from the DWBC.

[38] The thicknesses of the ceddies and aeddies were determined from the density field, but to associate them either with a ceddy or an æddy, we required them to have S and O_2 cores. The density profile at A15S station 111 does appear ceddy-like when compared to stations not in the unusual features commented here on A15S (Figure 8b (middle curve)), but there are no associated S or O_2 cores, and we did not attribute what was seen at A15S station 111 as due to a possible ceddy. In all cases the ceddies' and eddies' thicknesses were greater than those of their boluses. Their boluses were found in NADW, which in the Brazil Basin is found for 1200 m $\leq$ depths $\leq$ 3600 m [e.g., *Durrieu de Madron and Weatherly*, 1994]. While the boluses of the two ceddies extended downward to about 2600 m depth, that of the A15W eddy extended downward to about 3600 m depth. However, the portion of the A15W eddy bolus below about 2500 m depth was water found across a nearby front; how, when, and where it acquired this water is unclear. It thus appears that for depths down to about 2500 m the boluses of the ceddies and the A15W aeddy had properties of water associated with the DWBC of NADW.

[39] Several studies [e.g., *Hogg and Owens*, 1999; *Wienders et al.*, 2000] suggest that the transfer of NADW from the DWBC to the ocean interior mainly occurs in relatively narrow eastward currents. In Figure 11 the tongue-like salinity patterns at the equator, ~10°S, 20°–25°S, and ~35°S visualize this behavior. The shedding of eddies from the DWBC, as suggested by this study, appears as another mechanism for the eastward escape of NADW from the boundary. Thus the deep eddies should also contribute to the mixing of NADW with Circumpolar Deep Water that enters the South Atlantic at Drake Passage. From the deep float studies of *Richardson and Fratantoni* [1999] and *Hogg and Owens* [1999], deep eddies in the Brazil Basin appear to be common. However, from hydrographic studies they appear to be less so. Which view, that from deep floats or from hydrography, better reflects how common such features are is at present unclear. Until this point is better resolved the significance and implications of deep eddies for the NADW transport and in the circulation of the Brazil Basin remains to be determined.

Appendix A

[40] Figure A1 repeats Figures 5 and 6c with A15W station 87's data inserted halfway between stations 81 and 82. This simulates how the apparent features at these stations may have appeared just before they came into contact and suggests that what may have been sampled

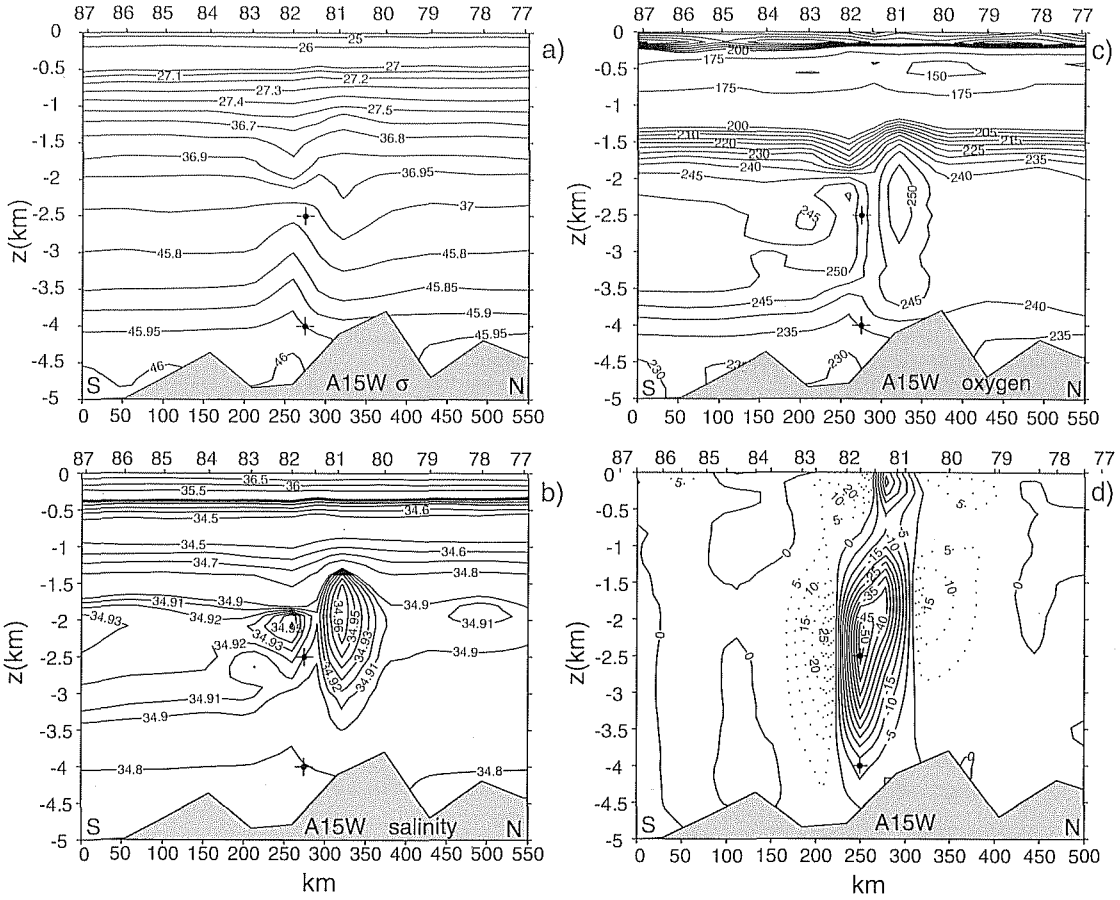

Figure A1. Section across stations 77–87 of A15W with station 87's data inserted halfway between stations 81 and 82 (see text): (a) density (as in Figure 3a), (b) S, (c) O_2, and (d) geostrophic velocity with the LNM at the bottom and positive into the plane of the figure. The dotted crosses denote where floats were set. S and N in the lower corners denote south and north.

was an aeddy and a ceddy in contact or shortly before coming into contact. Other stations' data were also inserted (see text).

[41] **Acknowledgments.** We have benefited from conversations with X. Carton, N. Hogg, D. Nof, J. McWilliams, and M. Stern and comments from two anonymous reviewers. We thank N. Hogg for graciously providing float data. R. Harkema helped with the figures. G. W. acknowledges support by the U.S. National Science Foundation under grants OCE92-06117 and OCE97-30120. The contributions of M. A. and H. M. were supported by IFREMER (grant 210161), INSU/CNRS, in the framework of the PNED. W. S. acknowledges support by NSF OCE 91-06835.

References

Ambar, I., et al., Outflows and overflows, paper presented at International Workshop on Outflows and Overflows in the Atlantic and Their Role in the Eastern Boundary Current System, Univ. of Lisbon, Lisbon, Portugal, 1991.

Bower, A. S., L. Ami, and I. Ambar, Lagrangian observations of Meddy formation during a Mediterranean Undercurrent Seeding Experiment, *J. Phys. Oceanogr.*, *27*, 2545–2575, 1997.

Brundage, L., and J. P. Dugan, Observations of an anticyclonic eddy of 18°C water in the Sargasso Sea (abstract), *Eos Trans. AGU*, *64*, 1019, 1983.

Colin de Verdière, A. C., H. Mercier, and M. Arhan, Mesoscale variability transition from the western to the eastern Atlantic and 48°N, *J. Phys. Oceanogr.*, *19*, 1149–1170, 1989.

Cornillon, P., D. Evans, and W. Large, Wamr outbreaks of the Gulf Stream in the Sargasso Sea, *J. Geophys. Res.*, *91*, 6583–6596, 1986.

Cresswell, G. R., The coalescence of two East Australian Current warm-core eddies, *Science*, *215*, 161–164, 1982.

D'Asaro, E., Observations of small eddies in the Beaufort Sea, *J. Geophys. Res.*, *92*, 6669–6684, 1988.

Durrieu de Madron, X., and G. Weatherly, Circulation, transport and bottom boundary layers of the deep currents in the Brazil Basin, *J. Mar. Res.*, *52*, 583–638, 1994.

Elliot, B. A., and T. B. Sanford, The subthermocline lens D1, I, Description of water properties and velocity profiles, *J. Phys. Oceanogr.*, *16*, 532–548, 1986.

Hogg, N. G., and W. B. Owens, Direct measurements of the deep circulation with the Brazil Basin, *Deep Sea Res., Part II*, *46*, 335–354, 1999.

Hogg, N. G., B. W Owens, G. Siedler, and W. Zenk, Circulation in the deep Brazil Basin, in *The South Atlantic: Present and Past Circulation*, edited by G. Wefer et al., pp. 249–260, Springer, New York, 1996.

Houry, S., E. Dombrowsky, P. de Mey, and J.-F. Minster, Brunt-Väisäilä frequency and Rossby radii in the South Atlantic, *J. Phys. Oceanogr.*, *17*, 1619–1626, 1987.

McWilliams, J. C., Submesoscale, coherent vortices in the ocean, *Rev. Geophys.*, *23*, 165–182, 1985.

Millot, C., Mesoscale and seasonal variability of the circulation in the western Mediterranean, *Dyn. Atmos. Oceans*, *15*, 179–214, 1991.

Nof, D., and W. K. Dewar, Alignment of lenses; laboratory and numerical experiments, *Deep Sea Res., Part I*, *41*, 1207–1229, 1994.

Paillet, J., M. Arhan, and M. S. McCartney, Spreading of the Labrador Sea Water in the eastern North Atlantic, *J. Geophys. Res.*, *103*, 10,225–10,239, 1998.

Polvani, L. M., Two-layer geostrophic vortex dynamics, part 2, Alignment and two-layer V-states, *J. Fluid Mech.*, *225*, 241–270, 1991.

Reid, J. L., On the total geostrophic circulation of the South Atlantic Ocean: Flow patterns, tracers, and transports, *Prog. Oceanogr.*, *23*, 149–244, 1989.

Richardson, P. L., Anticyclonic eddies generated near the Corner Rise Seamounts, *J. Mar. Res.*, *38*, 673–686, 1980.

Richardson, P. L., and D. M. Fratantoni, Float trajectories in the Deep Western Boundary Current and deep equatorial jets in the tropical Atlantic, *Deep Sea Res., Part II*, *46*, 305–334, 1999.

Richardson, P. L., and A. Tychensky, Meddy trajectories in the Canary Basin measured during the SEMAPHORE experiment, 1993–1995, *J. Geophys. Res.*, *103*, 25,029–25,046, 1998.

Sandoval, F., and G. Weatherly, Evolution of the Deep Western Boundary Current of Antarctic Bottom Water in the Brazil Basin, *J. Phys. Oceanogr.*, *31*, 1440–1460, 2001.

Schauer, U., A deep saline eddy in the West European Basin, *Deep Sea Res., Part A*, *36*, 1549–1565, 1989.

Schultz-Tokos, K. L., H.-H. Hinrichsen, and W. Zenk, Merging and migration of two meddies, *J. Phys. Oceanogr.*, *24*, 2129–2141, 1994.

Serra, N., and I. Ambar, Eddy generation in the Mediterranean Undercurrent, *Deep Sea Res.,Part II*, in press, 2002.

Shapiro, G. I., and S. L. Meschanov, Distribution and spreading of Red Sea Water and salt lens formation in the northwest Indian Ocean, *Deep Sea Res., Part I*, *38*, 21–34, 1991.

Speer, K. G., G. Siedler, and I. Talley, The Namib Col Current, *Deep Sea Res., Part I*, *42*, 1933–1950, 1995.

The Ring Group, Gulf Stream cold core rings: Their physics, chemistry and biology, *Science*, *212*, 1091–1100, 1981.

Weatherly, G. L., Y.-Y. Kim, and E. Kontar, Eulerian measurements of the Deep Western Boundary Current of North Atlantic Deep Water at 18°S, *J. Phys. Oceanogr.*, *30*, 971–986, 2000.

Wienders, N., M. Arhan, and H. Mercier, Circulation at the western boundary of the South and equatorial Atlantic: Exchanges with the ocean interior, *J. Mar. Res.*, *58*, 1007–1039, 2000.

M. Arhan and H. Mercier, Laboratoire de Physique des Océans (CNRS-IFREMER-UBO), IFREMER, Centre de Brest B.P.70, 29280 Plouzané, France.

W. Smethie Jr., Lamont-Doherty Earth Observatory, Palisades, NY 10964, USA.

G. Weatherly, Department of Oceanography, Florida State University, Tallahassee, FL 32306-4320, USA. (weatherly@ocean.fsu.edu)